ARTICLE
Journal of Cellular Biochemistry 116:1658–1667 (2015)

Journal of Cellular Biochemistry

The Osteogenic Priming of Mesenchymal Stem Cells is Impaired in Experimental Diabetes

J. C. Silva,[1] P. Sampaio,[2] M. H. Fernandes,[1] and P. S. Gomes[1]*

[1]*Laboratory for Bone Metabolism and Regeneration, Faculty of Dental Medicine, University of Porto, Rua Dr. Manuel Pereira da Silva, Porto 4200-393, Portugal*

[2]*Institute for Molecular Cell Biology (IBMC), Porto, Portugal*

ABSTRACT

Diabetes mellitus encompasses a group of metabolic conditions embracing the dysfunction and failure of various tissues and organs, including bone. Sustained bone alterations seem to result from anabolic, rather than catabolic processes, and suggest a decreased osteoblastic recruitment and activity. Current knowledge on the cellular and molecular mechanisms were provided by studies performed with osteogenic populations cultured in diabetic-simulated conditions, and osteogenic-induced precursor populations harvested from diabetic animals, sustaining an impaired cellular behavior in terms of osteogenic responsiveness and function. However, the reasons leaning to this impairment remain essentially unknown, as the priming capability and functionality of undifferentiated precursors, developed within the diabetic environment, have not been addressed. Accordingly, this work aims to evaluate the functionality and osteogenic priming capability of bone marrow-derived mesenchymal stem cells (MSCs), harvested from animals with experimental diabetes, and grown in the absence of any given differentiation factor. MSCs developed within a diabetic microenvironment displayed an impaired behavior, with diminished cell viability and proliferation, altered cytoskeleton organization, impaired osteogenic priming, and increased adipogenic activation. Further, the osteogenic induction of diabetic MSCs resulted in an impaired osteogenic commitment. The modified cell phenotype may be related, at least in part, with altered activity of ERK WNT and p38 signaling pathways in diabetic-derived cultures. Specific strategies, aiming the modulation of the verified hindrances, may be of therapeutic value to enhance the functionality of diabetic MSCs and sustain an improved outcome in the metabolism and regeneration of the bone tissue in diabetic conditions. J. Cell. Biochem. 116: 1658–1667, 2015.

KEY WORDS: DIABETES; BONE; MESENCHYMAL STEM CELLS; OSTEOGENIC DIFFERENTIATION

Diabetes mellitus (DM) encompasses a group of metabolic conditions characterized by chronic hyperglycemia occasioning from alterations in insulin secretion, action or both [Kuzuya et al., 2002]. The attained effects of DM embrace the dysfunction and failure of various tissues and organs, including bone [Van Belle et al., 2011]. Clinically, this seems to result in reduced bone mineral content, diminished linear bone growth, early onset of osteopenia and osteoporosis, increased risk of fragility fracture, and deficient bone healing [Retzepi and Donos, 2010].

In Type 1 DM (T1DM), particularly, a unswervingly reduced bone mineral density has been observed, broadly correlated with an increased risk of fragility fractures [Vestergaard, 2007]. Affected patients have inadequate accrual of peak bone mass, in which impaired bone formation seems to be the foremost contributor factor [Hofbauer et al., 2007]. In fact, studies conducted in experimental diabetic models and in cell culture systems sustain that bone alterations result from impaired anabolic, rather than enhanced catabolic processes [Massé et al., 2010].

Overall, T1DM and experimental diabetic conditions seem to be related to an impaired osteoblastic function that determines an imbalanced bone turnover, with associated alterations in the bone tissue quality. Current knowledge on the cellular and molecular mechanisms was provided by in vitro studies performed with osteogenic-induced normal precursor populations, cultured in diabetic-simulated conditions (i.e., hyperglycemic medium) [Brenner et al., 1992; Terada et al., 1998; Balint et al., 2001; Botolin and McCabe, 2006; Gopalakrishnan et al., 2006; Wang et al., 2010], which yielded information on the effect of high glucose levels on the osteogenic differentiation process, but failed to disclose the osteogenic capability of precursor populations arising within the diabetic environment. Therefore, alternative approaches were conducted with the assessment of osteogenic-induced precursor

*Correspondence to: Prof. Pedro Sousa Gomes, Faculty of Dental Medicine, University of Porto, Rua Dr. Manuel Pereira da Silva, Porto 4200-393, Portugal.
E-mail: pgomes@fmd.up.pt

Manuscript Received: 21 October 2014; Manuscript Accepted: 3 February 2015
Accepted manuscript online in Wiley Online Library (wileyonlinelibrary.com): 19 February 2015
DOI 10.1002/jcb.25126 • © 2015 Wiley Periodicals, Inc.

populations harvested from diabetic animals [Fulzele et al., 2010; Stolzing et al., 2010; Li et al., 2011; Tolosa et al., 2013], allowing data gathering on the ability of diabetes-derived precursors to respond to osteogenic stimuli. Conducted approaches revealed an impaired cellular behavior in terms of osteogenic responsiveness and function. However, the reasons leaning to this impairment remain essentially unknown. Within this context, this work aims to characterize the priming capability and functionality of undifferentiated precursor cells developed within the diabetic environment, an issue which has not been previously addressed. For that, bone marrow-derived mesenchymal stem cells (MSCs), harvested from animals with experimental diabetes induced with streptozotocin, STZ, (a relevant model of T1DM), were grown in the absence of any given differentiation factor. Established cultures were characterized for cell proliferation, viability/apoptosis, cytoskeleton organization, alkaline phosphatase activity, collagen synthesis, and osteogenic and adipogenic gene expression profile. Functional activity and osteogenic gene expression analyses were also conducted in osteogenic-induced MSCs. The activation of specific signaling pathways, namely the extracellular signal-regulated kinase (ERK), p38, and WNT was further evaluated in established cultures, as ERK and p38 are important for early osteoblast differentiation [Suzuki et al., 2002], whereas WNT signaling was found to favor osteoblastic precursor cells survival as well as the osteoblastic differentiation process [Almeida et al., 2005].

MATERIALS AND METHODS

ANIMALS

This study was conducted in accord with accepted standards of humane animal care, as outlined in the Ethical Guidelines. It was approved by *Direção Geral de Alimentação e Veterinária* and encompassed the standards for the protection of experimental animals, according to the Portuguese and European legislations. Briefly, 12 male Wistar rats (7–8 weeks old) were housed in groups and allowed food and water ad libitum, in accordance to home office regulations.

Experimental diabetes was induced by an intraperitoneal injection of STZ, Sigma® (60 mg/kg, in 10 mM citrate buffer, pH 4.5, n = 6)—STZ group. Control animals were injected with vehicle (n = 6)—control group. Hyperglycemia was confirmed 72 h after injection with a glucometer (Accu Check GO, Roche Diagnostics). Animals with blood glucose levels ≥300 mg/dl were considered to be diabetic. Six weeks following administration, animals were euthanized by exsanguination under general anesthesia (intraperitoneal injection of pentobarbital sodium 35 mg/kg).

DIABETIC BONE ALTERATIONS

Proximal tibial specimens were scanned by microcomputed tomography (μCT). μCT was performed in a μCT 35 (Scanco Medical), with a voxel size of 12 μm, X-ray tube voltage of 70 kVp, current intensity of 114 μA, and integration time of 600 ms. Structural evaluation of the trabecular content was carried out using the version 6.0 of the Scanco Medical software. Microstructural measures included bone volume per total volume (BV/TV), connective density (CD), trabecular number (Tb.N), trabecular thickness (Tb.Th), and trabecular separation (Tb.Sp). The computation of these structural measures has been previously detailed [Thomsen et al., 2005].

CELL CULTURES

Bone marrow-derived MSCs were isolated using modified versions of Dobson [Dobson et al., 1999] and Sekiya [Sekiya et al., 2002] methodologies, for bone marrow harvest and MSCs isolation, respectively. Briefly, femurs and tibias were excised, cleaned, and decontaminated. Following, epiphyses were cut off and diaphyses were flushed out with Rat-Mesenchymal Stem Cell Growth Medium (Lonza). Nucleated cells were isolated with a density gradient (Ficoll-Paque Premium®), re-suspended in culture medium, plated, and maintained in a humidified atmosphere (5% CO_2/air, 37°C) until ~70% confluence (~15 days). Cells were enzymatically released (trypsin 0.04%, 0.25% EDTA), and seeded at 10^4 cells/cm^{-2}. Cultures were maintained for 12 days and were assessed as follows.

CELL PROLIFERATION, METABOLIC ACTIVITY, APOPTOSIS, AND ALKALINE PHOSPHATASE ACTIVITY

Cell proliferation was estimated by the total DNA content, using the Quant-iT™ PicogreenVR DNA assay (Life technologies) according to the manufacturer's instructions, following cell lysis (Triton X-100 0.1%).

Metabolic activity was determined with the MTT assay. Cultures were incubated in standard conditions with MTT (0.5 mg/ml^{-1}, 4 h). Following, formazan crystals were dissolved and the absorbance was measured at 550 nm (Synergy HT, Biotek).

Apoptosis was quantified by measuring caspase-3 activity with the EnzCheck® Caspase-3 Assay Kit #2 (Molecular Probes), according to manufacturer's instructions.

Alkaline phosphatase (ALP) activity was determined in cell lysates, by the hydrolysis of p-nitrophenyl phosphate (30 min, 37°C) into p-nitrophenol, assessed at 405 nm (Synergy HT, Biotek). ALP was normalized to total protein content (measured according to the Lowry method). Results were presented as percentage of control.

CELL MORPHOLOGY

Cultures were stained for F-actin cytoskeleton and nucleus. Fixed cells (3.7% paraformaldehyde, 15 min) were permeabilized (0.1% Triton, 5 min), incubated with albumin (10 mg/ml^{-1}), and treated with Alexa Fluor 488®-conjugated phalloidin (1:20 dilution, 20 min) and propidium iodide (1 μg/ml^{-1}, 10 min). Cultures were observed by confocal laser scanning microscopy (CLSM, Leica SP2 AOBS; Leica Microsystems).

COLLAGEN SYNTHESIS

Assessment of the total collagen synthesis was conducted by in situ determination with Sirius red dye [Tullberg-Reinert and Jundt, 1999]. Briefly, fixed cultures were stained with 0.1% Sirius red solution (BDH, UK) in saturated picric acid (1 h), followed by rinsing with 0.01 N HCl. Collagen matrix was photodocumented before dissolving the stain in 0.1 N NaOH, 30 min. The absorbance was measured at 550 nm (Synergy HT, Biotek) and results were presented as percentage of staining compared to control.

GENE EXPRESSION

Cell cultures, at days 5 and 12, were analyzed by qPCR for the expression of housekeeping gene glyceraldehyde 3-phosphate dehydrogenase (*GAPDH*), *Alp*, Runt-related transcription factor 2 (*Runx2*), collagen type I alpha 1 (*Col1a1*), osteopontin (OPN), osteocalcin (OC), osteoprotegerin (OPG), peroxisome proliferator-activated receptors gamma (*Pparg*), insulin receptor substrate 1 (*Irs1*), insulin receptor substrate 2 (*Irs2*), and adipocyte protein 2 (ap2). Total RNA was extracted using the NucleoSpin® RNA II Kit (Macherey–Nagel), according to the manufacturer's instructions. Total RNA concentration and purity were assessed by UV spectrophotometry at 260 nm and by calculating $A_{260\,nm}/A_{280\,nm}$ ratio, respectively. RNA was reverse transcribed to cDNA using the SuperScript III First-Strand Synthesis System (Invitrogen). cDNA was amplified by real-time quantitative PCR using the SYBR Green RT-PCR kit (Applied Biosystems, Foster City, CA) in a Bio-Rad iCycler. Relative RNA levels were calculated using the iCycler software and normalized using GAPDH levels. The reaction was followed by melting curve analysis to verify specificity. The expression of each gene was evaluated using the 2-ΔΔCT method and dilution curves were used to test the PCR efficiency. Results were expressed as the percentage variation from control, corresponding to 100% at each time point. The primers used are listed in Table I.

OSTEOGENIC INDUCTION

Bone marrow-derived MSCs were isolated from Sham and STZ animals, as previously described. In order to address the capability of osteogenic induction of these populations, first passage cells were grown in osteogenic inducing conditions (α-MEM culture medium, supplemented with 10% fetal bovine serum, 50 μg/ml ascorbic acid, 4 mmol/L beta-glycerophosphate, and 10 nmol/L dexamethasone, all Sigma–Aldrich) for 12 days.

Cell cultures were characterized at day 5 and 12 for the expression of osteogenic-related genes *Alp*, *Runx2*, *Col1a1*, OPN, OC, OPG, as previously described, and normalized using GAPDH levels. Results were expressed as the percentage variation from control.

A histochemical assay (Alizarin Red) was further conducted to address the mineralization of the extracellular matrix of the grown cultures, at day 12, through the identification of calcium deposits within the matrix. Briefly, fixed cultures were covered with a 1% Alizarin Red S solution (0.028% in NH_4OH), pH 6.4, for 2 min, and were rinsed with distilled water and acid ethanol (ethanol, 0.01% HCL). Stained cultures were photo-documented with an inverted microscope (Nikon TMS) and a digital imaging system (Nikon DN100).

ACTIVATION OF SPECIFIC SIGNALING PATHWAYS IN STZ-DERIVED CULTURES

The activation of specific signaling pathways was evaluated in cultures grown in the presence of specific inhibitors. Briefly, at the eighth day of culture, established MSCs cultures were treated with 10 μM of the ERK inhibitor PD 98059 (Sigma–Aldrich), 10 μM of the WNT inhibitor ICG-001 (R&D Systems), or 20 μM of the p38-inhibitor SB203580 (Sigma–Aldrich), for the last 6 h of the culture. These were characterized for metabolic activity and gene expression analysis, as described above. The expression levels of *Alp*, *Runx2* (two relevant osteogenic markers with distinct transcription control), and *Pparg* (a transcription factor associated with adipogenic commitment) were assayed. Results were presented as percentage of variation from control.

STATISTICAL ANALYSIS

Three independent experiments were performed with the cell cultures established from different animals. In quantitative assays, each point represents the mean ± standard error of six replicates. Statistical analysis was done by two-way analysis of variance (ANOVA) followed by Tukey range test post hoc analysis. *P*-values ≤ 0.05 were considered significant.

RESULTS

STZ-INDUCED DIABETIC MODEL

Animals of the control group revealed an increased body weight (6.41% ± 3.45), while animals of the STZ group lost weight (37.57% ± 8.65), during the experimental period. At euthanasia, STZ group had a significantly higher glycemia (377.3 mg/dl ± 20.2), as compared to control (≤125 mg/dl).

The microtomographic evaluation of the proximal tibia revealed a reduced trabecular content in STZ animals (Fig. 1, right). As compared to control (Fig. 1, left), a decreased trabecular interconnectivity was verified at the bone's proximal methaphysis. Morphometric indexes of the trabecular structure revealed a significant decrease in BV/TV and in trabecular thickness, and a tendency for the reduction of the connective density. No significant

TABLE I. Forward and Reverse Sequences of the Used Primers for the qPCR Analysis

Gene	Forward sequence	Reverse sequence
GAPDH	AAATGGTGAAGGTCGGTGTG	CCCATACCCACCATCACACC
ALP	GGCTCTGCCGTTGTTTC	GGGTTGGGTTGAGGGACT
RUNX-2	ATCCAGCCACCTTCACTTACACC	GGGACCATTGGGAACTGATAG
Collagen 1A1	TGGCAAGAACGGAGATGA	AGCTGTTCCAGGCAATCC
Osteopontin	AAAAATGCTCACCATCACTGC	AATTGCCACACTGACTTCCAC
Osteocalcin	GCCCTGACTGCATTCTGCCTCT	TCACCACCTTACTGCCCTCCTG
Osteoprotegerin	ATTGGCTGAGTGTTCTGGT	CTGGTCTCTGTTTTGATGC
PPAR-γ	GCGGAGATCTCCAGTGATATC	TCAGCGACTGGGACTTTTCT
IRS-1	TGTGCCAAGCAACAAGAAAG	ACGGTTTCAGAGCAGAGGAA
IRS-2	GAGCCTTCAGTAGCCACAGG	CAGGCGTGGTTAGGGAGTAA
aP2	ATGTGTCATGAAAGGCGTGA	AAACCACCAAATCCCATCA

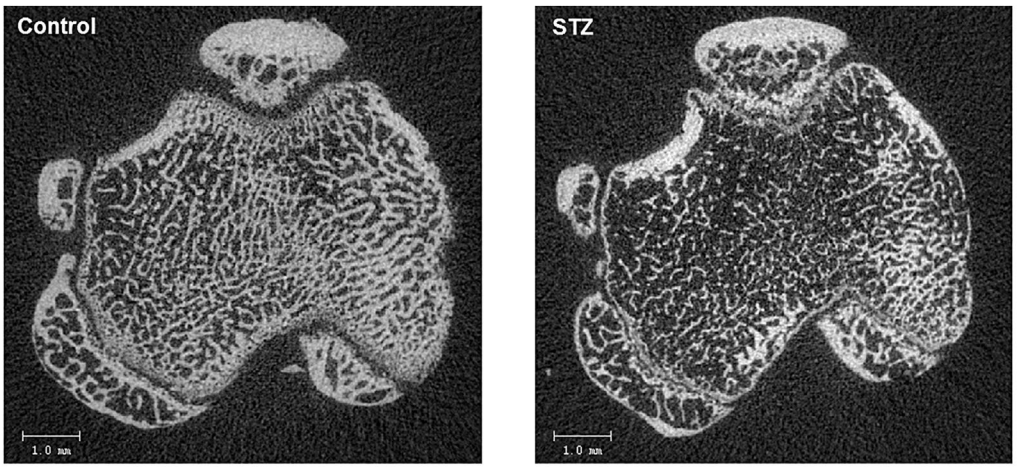

	BV/TV	CD	Tb.N	Tb.Th	Tb.Sp
Control	0.277 ± 0.008	106.770 ± 7.08	4.338 ± 0.057	0.081 ± 0.0034	0.223 ± 0.007
STZ	0.188* ± 0.014	98.53 ± 8.05	4.402 ± 0.288	0.065* ± 0.0018	0.221 ± 0.014

Fig. 1. Top: representative 2D microtomographic images of the proximal tibia methaphysis, in control and STZ animals (n = 6). Bottom: microstructural parameters of the trabecular structure of the proximal tibia. Assessed variables included BV/TV (bone volume per total volume), CD (connective density), Tb.N (trabecular number), Tb.Th (trabecular thickness), and Tb.Sp (trabecular separation). *: significantly different from control ($P \leq 0.05$).

differences were found regarding trabeculae number and trabeculae separation (Fig. 1; Table I).

CELL BEHAVIOR

Cell proliferation, metabolic activity, apoptosis, and alkaline phosphatase. Data on the assessed cellular functions, expressed as the percentage variation from control, are summarized in Figure 2. Briefly, in comparison to control, STZ-derived cultures presented reduced total DNA content from day 5 onwards. Significant differences were attained at both days 8 and 12 of the culture. Regarding the assessment of the cultures' metabolic activity, STZ-derived cultures attained higher MTT reduction values at early culture time points (days 1 and 5, with no significant differences) despite that, at days 8 and 12, a significant reduction was verified, as compared to control. Apoptosis was estimated by the determination of caspase-3 activity and, in comparison to control, STZ-derived cultures attained a significant higher caspase-3 activity, at days 8 and 12. ALP activity was assayed from day 5 onwards. Compared to control, cultures from STZ animals presented an increased enzyme activity, which was found to be significantly higher at days 8 and 12.

Cell morphology. CLSM images are shown in Figure 3. In control cultures, at 3 days, cells presented a characteristic morphology with elongated cytoplasm and a dense network of microfilaments and stress fibers. Strong labeling was often observed along the cellular edge and within the extended cellular filopodia. Cells exhibited intense cell-to-cell contacts and a characteristic nodular growth pattern. Throughout time, cells proliferated actively and organized into multilayers.

STZ-derived cultures presented a similar behavior despite that, at 3 days, fewer long stress fibers were visible on proliferating cells, and the intense labeling at the cellular edge, broadly verified in control, was more rarely observed. Nevertheless, cells proliferated actively and reached multilayer organization, in a similar fashion to control.

Collagen. Data on the total collagen production are presented in Figure 4. Histochemical analysis revealed the cluster organization of the cultures at early time points, with progressive organization into multilayers through the culture period. Collagen content increased in both control and STZ-derived cultures through time. Comparatively, STZ cultures presented decreased staining intensity, particularly noticeable at day 12. The quantitative determination of stained products revealed a reduction in STZ cultures, which was significant at day 12.

Osteogenic gene expression of undifferentiated cultures. Results addressing the osteogenic gene expression are presented in Figure 5A. In undifferentiaing conditions, STZ cultures presented increased *Alp* expression, but decreased expression of other assayed osteogenic markers (*Runx2*, *Col1a1*, osteopontin, osteocalcin, and osteoprotegerin), both at day 5 and 12, as compared to control.

Adipogenic gene expression of undifferentiated cultures. Results addressing the adipogenic gene expression are presented in Figure 5B. STZ-derived cultures, grown in undifferentiating conditions, revealed significantly increased expression of *Pparg*, *Irs1*, and *Irs2*, at both days 5 and 12 of the culture, but expression of ap2 was not significantly affected.

Osteogenic induction of MSCs cultures. Results regarding the osteogenic induction of undifferentiated MSCs cultures are

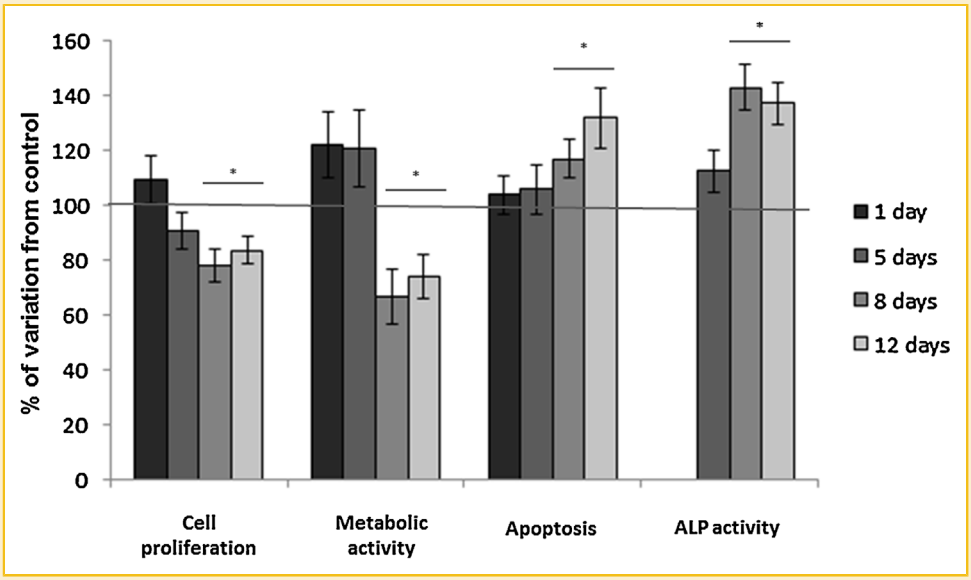

Fig. 2. Cell proliferation (DNA assay), metabolic activity (MTT assay), apoptosis (caspase-3 activity), and alkaline phosphatase activity (ALP) of MSCs cultures, established for 12 days, from control and STZ-induced diabetic animals (n = 6). Results were expressed as the percentage variation from control corresponding to 100% at each time point. *: significantly different from control ($P \leq 0.05$).

presented in Figure 5A (gene expression analysis) and Supplemental Figure S1 (extracellular matrix mineralization). Following osteogenic induction, STZ cultures presented an impaired expression of all the assayed osteogenic-related genes (i.e., *Alp*, *Runx2*, *Col1a1*, osteopontin, osteocalcin, and osteoprotegerin). Furthermore, at day 12 of the cultures, a significant decreased mineralization of the extracellular matrix, as assessed by the Alizarin Red assay, was verified in STZ-derived cultures.

Activation of specific signaling pathways. Data on the activation of signaling pathways are presented in Figure 6. Briefly, inhibition

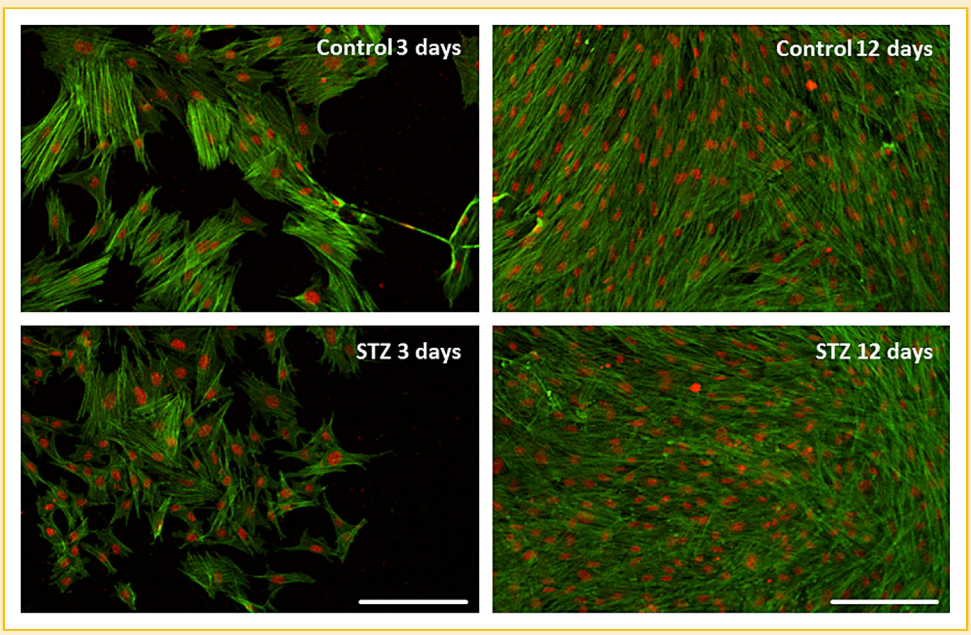

Fig. 3. Representative confocal laser scanning microscopy images of MSCs, established for 3 and 12 days, from control and STZ-induced diabetic animals (n = 6). Cytoskeleton was stained in green and nucleus counterstained in red. Scale bar corresponds to 200 μm.

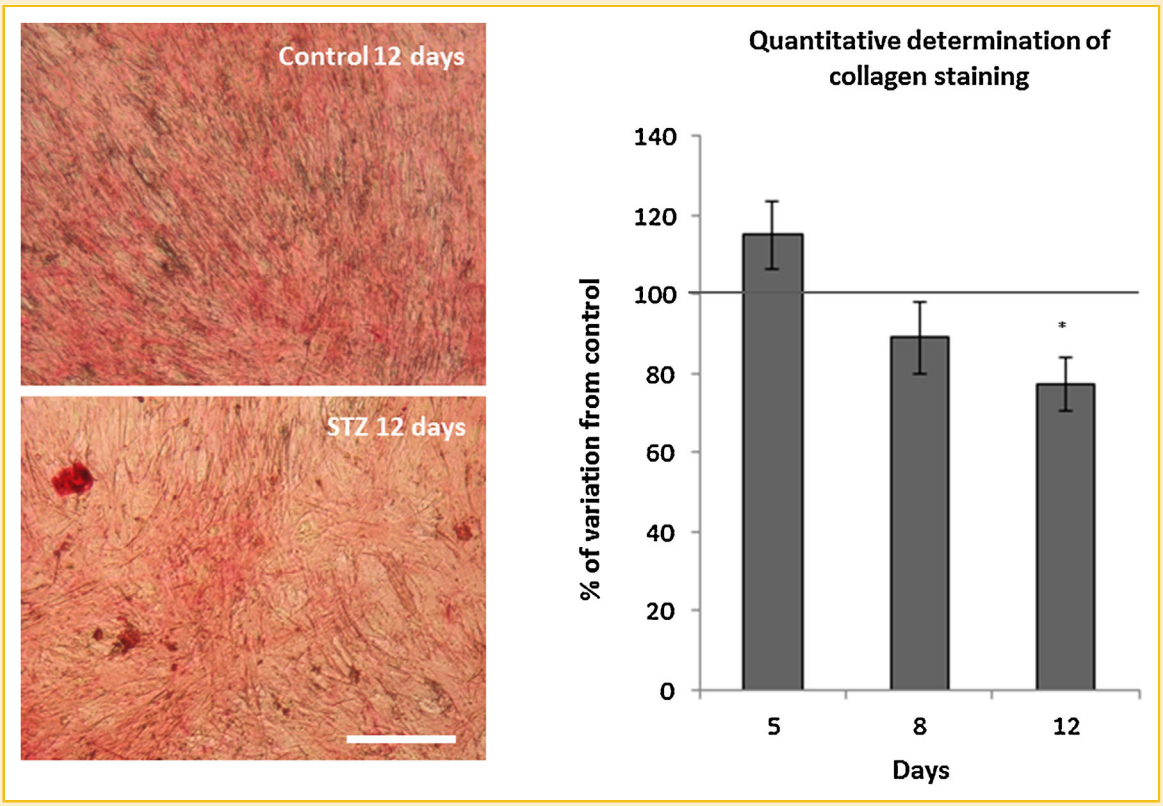

Fig. 4. Left: total collagen staining of MSCs cultures, established for 12 days, from control and STZ-induced diabetic animals (n = 6). Scale bar corresponds to 750 μm. Right: colorimetric determination of the total collagen stained products within the established MSCs cultures. Results were expressed as the percentage variation from control corresponding to 100% at each time point. *: significantly different from control ($P \leq 0.05$).

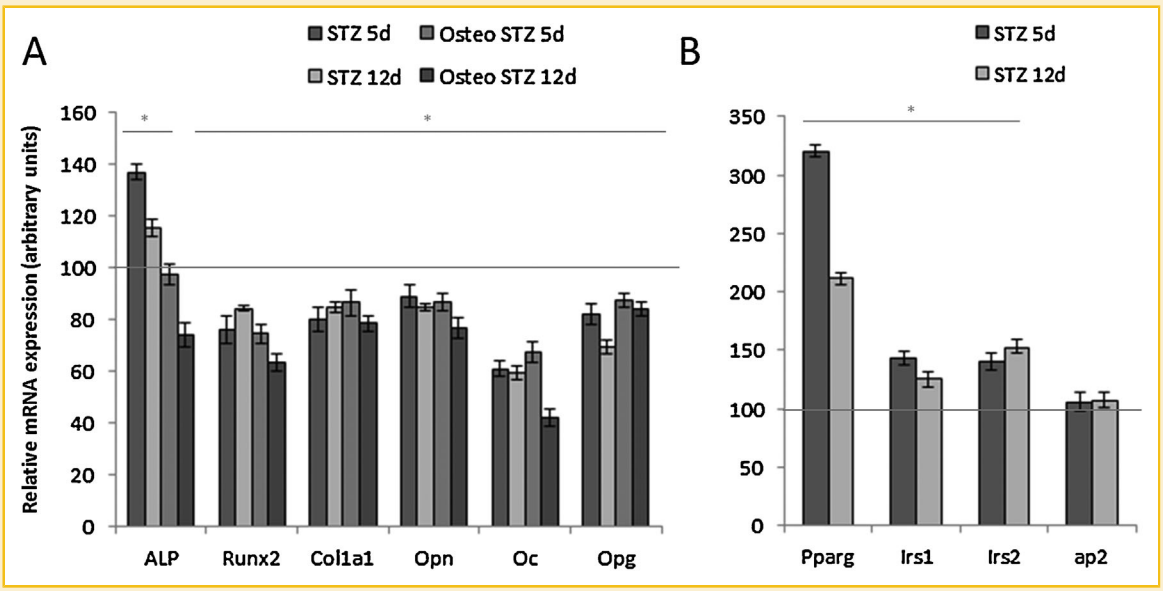

Fig. 5. A: qPCR gene expression analysis of *Alp*, *Runx2*, *Col1a1*, osteopontin (Opn), osteocalcin (Oc), osteoprotegerin (Opg), in MSCs cultures, established for 5 and 12 days, from control and STZ-induced diabetic animals (n = 6). Cultures were grown in undifferentiating (STZ) and osteogenic-differentiating (Osteo STZ) conditions. B: qPCR gene expression analysis of Pparg, Irs1, Irs2, and ap2, in undifferentiated STZ-derived MSCs cultures, established for 5 and 12 days. Results were expressed as the percentage variation from control corresponding to 100% at each time point. *: significantly different from control ($P \leq 0.05$).

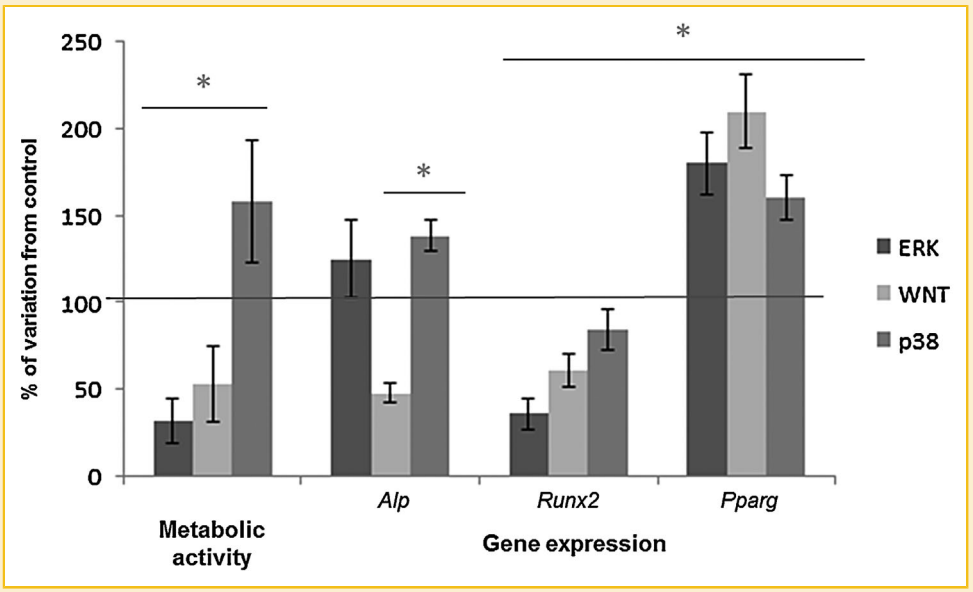

Fig. 6. Metabolic activity and gene expression analysis (of *Alp*, *Runx2*, and *Pparg*) of MSCs cultures, from control and STZ-induced diabetic animals, grown for 8 days. Cultures were incubated with specific inhibitors of the ERK (PD 98059), p38 (SB203580), and WNT (ICG-001) signaling pathways for the last 6 h of culture ($n = 6$). Results were expressed as the percentage variation from control corresponding to 100%. *: significantly different from control ($P \leq 0.05$).

studies with pathway specific inhibitors revealed that, comparing to control, STZ-derived cultures presented reduced metabolic activity regarding ERK and WNT activation, while an increased metabolic activity was verified within p38 assessment. Regarding the evaluation of *Alp* expression, in STZ-derived cultures, increased levels were verified to be associated with ERK and p38 pathways, while a significant reduced expression was found to be associated with WNT pathway. Furthermore, in diabetic-derived cultures, *Runx2* expression was consistently reduced, and *Pparg* levels were significantly increased within the experiments conducted for the evaluation of three pathways activation.

DISCUSSION

Diabetic conditions seem to play a negative role on bone tissue metabolism and regeneration, even though little is known regarding the determinant molecular and cellular mechanisms affecting the maturation and functional activity of osteoblastic precursor populations. This study focused on the characterization of the behavior of unstimulated MSCs developed within a diabetic environment, an issue that was not addressed before. MSCs were harvested from the bone marrow of diabetic animals and allowed to adhere and to expand in vitro, under undifferentiating conditions (i.e., in the absence of supplemented lineage-specific growth factors or diabetic-simulated conditions). Attained results support the notion that bone marrow-derived MSCs, developed under the diabetic microenvironment, display an impaired viability/proliferation, increased apoptosis, and diminished osteogenic and increased adipogenic priming. Furthermore, osteogenic induction of these cells, further confirmed the impaired osteogenic commitment, in comparison to those grown from non-diabetic animals.

Within the used animal model, diabetic induction with STZ allowed the development of hyperglycemia (plasma glucose $\geq$300 mg/dl), with associated body weight decrease, and changes in the bone structure. Microtomographic evaluation of the proximal tibia showed significant morphological alterations and reduced morphometric indexes (i.e., decreased BV/TV and trabecular thickness), supporting the development of an hyperglycemia-mediated osteopenic condition [Silva et al., 2009].

MSCs cultures from diabetic animals, at late culture time points, revealed an increased apoptotic rate, impaired proliferation—reduced total DNA content—and a reduced metabolic activity, which may be related with the reduced number of active cells in STZ-derived cultures. This behavior was similar to the one verified within in vitro models mimicking the diabetic microenvironment, such as hyperglycemia and hypoinsulinemia [Terada et al., 1998; Botolin and McCabe, 2006; Gopalakrishnan et al., 2006; Fulzele et al., 2010], reporting an impaired proliferation of osteoblastic populations. Also, an increased apoptosis was verified in dexamethasone-induced osteoblastic differentiating MSCs from diabetic animals [Stolzing et al., 2010]. These alterations may be related to a deficient insulin receptor activation by insulin, which induces a mitogenic stimulation, coupled with the inhibition of apoptosis, in a process probably mediated by the downregulation of p27 (a cyclin-dependent kinase inhibitor that seems to attenuate cell proliferation) [Thrailkill et al., 2005]. Other osteotropic factors produced by pancreatic β cells, such as islet amyloid polypeptide and preptin (which are absent or significantly reduced in diabetic conditions), also seem to favor osteoblastic proliferation and to reduce the frequency of apoptotic events [Bosetti et al., 2013].

In terms of cytoskeleton organization, at 3 days, STZ-derived cultures presented a reduced number of stress fibers and decreased F-

actin labeling at the cell border. This is line with previous observations in MSCs grown from diabetic mice, revealing a decreased adhesion to substrate, and a disturbed distribution and expression of F-actin, leading to abnormal stress fibers formation [Li et al., 2011]. The cytoskeleton organization is critical for cell morphology and homeostasis, notwithstanding its involvement in other cellular processes such as intracellular transport and differentiation [Wang et al., 1993]. Osteoblastic function is highly dependent upon cell adhesion and cytoskeletal organization, as extracellular cues seem to direct MSCs functionality and, particularly, the osteogenic differentiation [Kilian et al., 2010].

Grown MSCs from STZ animals revealed an increased ALP activity and an impaired collagen production at late culture time points. Increased ALP activity was previously described in osteoblastic cells grown in vitro, in chronic hyperglycemic conditions [Balint et al., 2001; Botolin and McCabe, 2006], and in the serum of diabetic patients [Goldberg et al., 1977; Massé et al., 2010]. Nonetheless, it has been suggested that ALP within the diabetic environment presents an altered kinetic profile, supposedly in a process related to changes in metal-binding properties [Rezende et al., 1993; Fernandes et al., 1999]. Regarding collagen expression in diabetic conditions, a significant reduction of total collagen was verified in the bone of diabetic rats [Spanheimer et al., 1988]. Furthermore, collagen synthesis of human osteoblasts was significantly reduced in the presence of human diabetic serum [Brenner et al., 1992]. The high level of pro-inflammatory cytokines verified within the diabetic environment [Goldberg, 2009] may contribute to the altered ALP/collagen expression, as tumor necrosis factor α and interleukin 1β were found to stimulate ALP activity and lessen collagen expression in human MSCs [Ding et al., 2009].

Regarding MSCs gene expression profile, normally, this population expresses a genetic signature of its potential multilineage differentiation capacity, even at early differentiating stages [Seshi et al., 2000]. In the present work, MSCs harvested from diabetic animals presented an altered gene expression profile. In STZ-derived cultures, the osteogenic-related gene expression revealed an increased *Alp* expression, and a decreased expression of *Runx2*—the master regulator of the osteogenic differentiation—and, as well, a decreased expression of several of its downstream targets (i.e., *Col1a1*, osteopontin, osteocalcin, osteoprotegerin). This is an interesting finding supporting that the diabetic microenvironment may hinder RUNX2 activity and downregulate the expression of its downstream targets. *Alp* expression, found to be increased in STZ cultures, and thus sustaining its acknowledged increased activity, seems to be independently regulated from RUNX2 activation. This comes in line with previous data on the inhibition of RUNX2, with either small interfering RNA [Kotobuki et al., 2008], or over-expression of a dominant negative [Ding et al., 2009], which were found not to alter *Alp* expression, and suggested that it may be unrelated to this transcription factor regulation. Additionally, gene expression analyses were also conducted on osteogenic-induced MSCs. Cultures from STZ-derived animals revealed an impaired osteogenic induction, both at days 5 and 12, with significantly reduced expression of both *Alp* and *runx2*, as well as its assayed downstream targets, thus validating the compromised osteogenic priming of undifferentiated precursors. In accordance, a reduced mineralization of the extracellular matrix—the summit of the osteogenic differentiation process—was further verified in STZ-derived cultures through Alizarin Red staining. The impaired osteogenic capability of differentiating diabetic MSCs has been previously established in both in vitro [Zhao et al., 2013] and in vivo [Lu et al., 2003; Fowlkes et al., 2008].

Additionally, in undifferentiated MSCs from diabetic animals, expression of the adipogenic markers *Pparg*, *Irs1,* and *Irs2* was significantly upregulated, while the expression of *ap2* was not affected. PPARG is a key regulator of adipogenic differentiation and shifts the balance of MSCs fate by favoring adipocyte differentiation and thus, inhibiting osteoblast differentiation [Wan, 2010]. An increased expression of *Pparg* has been verified in osteoblastic cells grown in hyperglycemic conditions [Wang et al., 2010] and in growing osteoblasts from diabetic animals [Tolosa et al., 2013]. Results on the present work suggest that the enhanced adipogenic priming might be related to the up-regulation of IRS-1 and IRS-2, since the activation of these adapter proteins and associated PI 3-kinase pathway were found to be determinant for the activation of PPARG, resulting in the induction of adipogenic differentiation [Muruganandan et al., 2009]. Most interestingly, the expression of *ap2*, abundantly synthesized in the late phase of developing adipocytes [Muruganandan et al., 2009], was found not to differ significantly between growing STZ and control-derived MSCs cultures. This seems to support an increased priming of the adipogenic trigger by diabetic-derived MSCs, without an effective progression into this differentiation pathway.

The assessment of significant signaling pathways revealed a reduced metabolic activity associated with ERK and WNT signaling, in STZ-derived MSCs cultures. Furthermore, a different regulation on the assayed osteogenic markers was verified in diabetic-derived cultures, as *Alp* expression was found to be enhanced by p38 pathway and diminished by WNT pathway; while ERK, WNT, and p38 pathways converged to a decreased expression of *Runx2*. Contrariwise, *Pparg* levels were found to be increased in STZ-derived cultures, in close association with the three assayed pathways.

These results are in accordance with previous literature data on the activity of the different signaling pathways. ERK pathway activation was shown to be crucial for the regulation of cell proliferation, and also to play a determining role in the differentiation of MSCs [Augello and Bari, 2010]. Briefly, the specific inhibition of this pathway was found to block the osteogenic differentiation of human MSCs and to induce the adipogenic differentiation of these cells [Jaiswal et al., 2000]. ERK activation was thus found to stimulate osteoblastic-specific gene expression through RUNX2 activation [Ge et al., 2009]. Of additional relevance, insulin and insulin-like growth factor 1, known to be reduced on the diabetic milieu, was found to induce osteoblast proliferation and differentiation via ERK activation [Zhang et al., 2012].

WNT signaling has also been associated with the osteogenic commitment and adipogenic repression of precursor cells, namely by the stimulation of RUNX2 and downregulation of PPARG, respectively [Takada et al., 2009]. In this work, the expression of both osteogenic markers, *Alp,* and *Runx2*, was downregulated in

association with WNT signaling, while the expression of *Pparg* was enhanced, in STZ-derived cultures, thus sustaining an impaired activation of this signaling pathway. In type I diabetes, a decreased osteoblastogenesis was found to be associated with the inhibition of WNT pathway [Hie et al., 2011]; while hyperglycemia was found to target distinct components of the WNT pathway in osteoblasts, leading to its inhibition [López-Herradón et al., 2013], in a process mediated, at least in part, by the increased activation of p38 pathway [Suzuki et al., 2002].

In the present study, the metabolic activity of the STZ-derived cultures was found to be enhanced through p38 activation, which was also associated with an increased *Alp* and *Pparg* expression. p38 activation was previously found to specifically increase *Alp* expression in osteoblastic populations, despite its negative association with the osteoblastic differentiation process [Suzuki et al., 2002; Hager et al., 2009]. This correlates with the findings of the present research in which an increased *Alp* expression and activity were verified in STZ-derived MSCs cultures, regardless of the reduced *Runx2* activity and impaired osteogenic priming. Furthermore, within the diabetic milieu, an increased activation of p38 has been verified, through different signaling approaches and cellular populations [Igarashi et al., 1999], thus supporting an increased p38 activity within STZ-derived cultures.

Generally, MSCs developed within a diabetic microenvironment, and cultured in undifferentiating conditions, displayed an impaired functionality, with diminished cell proliferation and increased apoptosis. Furthermore, an altered cytoskeleton organization, increased ALP activity, and decreased collagen synthesis were verified. In terms of gene expression, altered osteogenic gene profile was verified, with decreased expression of Runx2 and several of its downstream targets; while increased adipogenic gene expression was attained. Furthermore, the osteogenic-induction of cultured STZ-derived MSCs confirmed the impaired osteogenic phenotype, through gene expression analysis and assessment of the extracellular mineralization process. Overall, this behavior is consistent with an impaired osteogenic priming of bone marrow-derived undifferentiated MSCs, that can be associated with the maintenance of a less mature phenotype of this population [Stein et al., 1990]. In agreement, a deficiency in the conversion of immature mesenchymal cells to mature osteoblasts was verified in a marrow ablation model of diabetic mice [Lu et al., 2003]. Assessment of relevant signaling pathways revealed a decreased activity of ERK and WNT, and an increased signaling through p38, which may determine, at least in part, the verified functional hindrances.

Results of the present study suggest for the first time that the diabetic environment may alter MSCs signaling and functionality, that appears to be intrinsic and long-lasting. These might contribute to the acknowledged diabetic-associated bone alterations, as verified by the impaired behavior of osteogenic-induced precursor populations from diabetic animals, within the bone tissue of animal models of experimental diabetes and in clinical trials with diabetic patients. In this way, local or systemic strategies, specifically targeted to modulate the verified hindrances, may improve the functionality of MSCs in diabetic conditions, and sustain an improved outcome in the metabolism and regeneration of the bone tissue in diabetic conditions.

REFERENCES

Almeida M, Han L, Bellido T, Manolagas S, Kousteni S. 2005. Wnt proteins prevent apoptosis of both uncommitted osteoblast progenitors and differentiated osteoblasts by β-catenin-dependent and -independent signaling cascades involving src/erk and phosphatidylinositol 3-kinase/akt. J Biol Chem 280(50):41342–41351.

Augello A, Bari C. 2010. The regulation of differentiation in mesenchymal stem cells. Hum Gene Ther 21:1226–1238.

Balint E, Szabo P, Marshall C, Sprague S. 2001. Glucose-induced inhibition of in vitro bone mineralization. Bone 28(1):21–28.

Bosetti M, Sabbatini M, Nicolì E, Fusaro L, Cannas M. 2013. Effects and differentiation activity of IGF-I, IGF-II, insulin and preptin on human primary bone cells. Growth Factors 31:57–65.

Botolin S, McCabe L. 2006. Chronic hyperglycemia modulates osteoblast gene expression through osmotic and non-osmotic pathways. J Cell Biochem 99:411–424.

Brenner R, Riemenschneider B, Blum W, Mörike M, Teller W, Pirsig W, Heinze E. 1992. Defective stimulation of proliferation and collagen biosynthesis of human bone cells by serum from diabetic patients. Acta Endocrinol-Cop 127(6):509–514.

Ding J, Ghali O, Lencel P, Broux O, Chauveau C, Devedjian J, Hardouin P, Magne D. 2009. TNF-α and IL-1β inhibit RUNX2 and collagen expression but increase alkaline phosphatase activity and mineralization in human mesenchymal stem cells. Life Sci 84:499–504.

Dobson K, Reading L, Haberey M, Marine X, Scutt A. 1999. Centrifugal isolation of bone marrow from bone: an improved method for the recovery and quantitation of bone marrow osteoprogenitor cells from rat tibiae and femurae. Calcified Tissue Int 65:411–413.

Fernandes S, Furriel R, Petenusci S, Leone F. 1999. Streptozotocin-induced diabetes: significant changes in the kinetic properties of the soluble form of rat bone alkaline phosphatase. Biochem Pharmacol 58:841–849.

Fowlkes JL, Bunn RC, Liu L, Wahl EC, Coleman HN, Cockrell GE, Perrien DS, Lumpkin CK, Thrailkill KM. 2008. Runt-related transcription factor 2 (RUNX2) and RUNX2-related osteogenic genes are down-regulated throughout osteogenesis in type 1 diabetes mellitus. Endocrinology 149:1697–1704.

Fulzele K, Riddle RC, DiGirolamo DJ, Cao X, Wan C, Chen D, Faugere M-C, Aja S, Hussain MA, Brüning JC. 2010. Insulin receptor signaling in osteoblasts regulates postnatal bone acquisition and body composition. Cell 142: 309–319.

Ge C, Xiao G, Jiang D, Yang Q, Hatch NE, Roca H, Franceschi RT. 2009. Identification and functional characterization of ERK/MAPK phosphorylation sites in the Runx2 transcription factor. J Biol Chem 284: 32533–32543.

Goldberg D, Martin J, Knight A. 1977. Elevation of serum alkaline phosphatase activity and related enzymes in diabetes mellitus. Clin Biochem 10:8–11.

Goldberg R. 2009. Cytokine and cytokine-like inflammation markers, endothelial dysfunction, and imbalanced coagulation in development of diabetes and its complications. J Clin Endocrinol Metab 94:3171–3182.

Gopalakrishnan V, Vignesh RC, Arunakaran J, Aruldhas MM, Srinivasan N. 2006. Effects of glucose and its modulation by insulin and estradiol on BMSC differentiation into osteoblastic lineages. Biochem Cell Biol 84(1):93–101.

Hager S, Lampert F, Orimo H, Stark G, Finkenzeller G. 2009. Up-regulation of alkaline phosphatase expression in human primary osteoblasts by cocultivation with primary endothelial cells is mediated by p38 mitogen-activated protein kinase-dependent mRNA stabilization. Tissue Eng Part A 15: 3437–3447.

Hie M, Iitsuka N, Otsuka T, Tsukamoto I. 2011. Insulin-dependent diabetes mellitus decreases osteoblastogenesis associated with the inhibition of Wnt signaling through increased expression of Sost and Dkk1 and inhibition of Akt activation. Int J Mol Med 28:455–462.

Hofbauer LC, Brueck CC, Singh SK, Dobnig H. 2007. Osteoporosis in patients with diabetes mellitus. J Bone Miner Res 22:1317–1328.

Igarashi M, Wakasaki H, Takahara N, Ishii H, Jiang Z-Y, Yamauchi T, Kuboki K, Meier M, Rhodes CJ, King GL. 1999. Glucose or diabetes activates p38 mitogen-activated protein kinase via different pathways. J Clin Invest 103(2):185–195.

Jaiswal R, Jaiswal N, Bruder S, Mbalaviele G, Marshak D, Pittenger M. 2000. Adult human mesenchymal stem cell differentiation to the osteogenic or adipogenic lineage is regulated by mitogen-activated protein kinase. J Biol Chem 275:9645–9652.

Kilian KA, Bugarija B, Lahn BT, Mrksich M. 2010. Geometric cues for directing the differentiation of mesenchymal stem cells. Proc Natl Acad Sci USA 107:4872–4877.

Kotobuki N, Matsushima A, Kato Y, Kubo Y, Hirose M, Ohgushi H. 2008. Small interfering RNA of alkaline phosphatase inhibits matrix mineralization. Cell Tissue Res 332:279–288.

Kuzuya T, Nakagawa S, Satoh J, Kanazawa Y, Iwamoto Y, Kobayashi M, Nanjo K, Sasaki A, Seino Y, Ito C, Shima K, Nonaka K, Kadowaki T. 2002. Report of the Committee on the classification and diagnostic criteria of diabetes mellitus. Diabetes Res Clin Pract 55:65–85.

Li L, Xia Y, Wang Z, Cao X, Da Z, Guo G, Qian J, Liu X, Fan Y, Sun L, Sang A, Gu Z. 2011. Suppression of the PI3K–Akt pathway is involved in the decreased adhesion and migration of bone marrow-derived mesenchymal stem cells from non-obese diabetic mice. Cell Biol Int 35:961–966.

López-Herradón A, Portal-Núñez S, García-Martín A, Lozano D, Pérez-Martínez FC, Ceña V, Esbrit P. 2013. Inhibition of the canonical Wnt pathway by high glucose can be reversed by parathyroid hormone-related protein in osteoblastic cells. J Cell Biochem 114(8):1908–1916.

Lu H, Kraut D, Gerstenfeld L, Graves D. 2003. Diabetes interferes with the bone formation by affecting the expression of transcription factors that regulate osteoblast differentiation. Endocrinology 144:346–352.

Massé P, Pacifique M, Tranchant C, Arjmandi B, Ericson K, Donovan S, Delvin E, Caissie M. 2010. Bone metabolic abnormalities associated with well-controlled type 1 diabetes (IDDM) in young adult women: a disease complication often ignored or neglected. J Am Coll Nutr 29:419–429.

Muruganandan S, Roman A, Sinal C. 2009. Adipocyte differentiation of bone marrow-derived mesenchymal stem cells: cross talk with the osteoblastogenic program. Cell Mol Life Sci 66:236–253.

Retzepi M, Donos N. 2010. The effect of diabetes mellitus on osseous healing. Clin Oral Implants Res 21:673–681.

Rezende A, Petenusci S, Urbinati E, Leone F. 1993. Kinetic properties of osseous plate alkaline phosphatase from diabetic rats. Comp Biochem Physiol Comp Physiol 104:469–474.

Sekiya I, Larson BL, Smith JR, Pochampally R, Cui JG, Prockop DJ. 2002. Expansion of human adult stem cells from bone marrow stroma: conditions that maximize the yields of early progenitors and evaluate their quality. Stem cells 20:530–541.

Seshi B, Kumar S, Sellers D. 2000. Human bone marrow stromal cell: coexpression of markers specific for multiple mesenchymal cell lineages. Blood Cells Mol Dis 26:234–246.

Silva MJ, Brodt MD, Lynch MA, McKenzie JA, Tanouye KM, Nyman JS, Wang X. 2009. Type 1 diabetes in young rats leads to progressive trabecular bone loss, cessation of cortical bone growth, and diminished whole bone strength and fatigue life. J Bone Miner Res 24:1618–1627.

Spanheimer R, Umpierrez G, Stumpf V. 1988. Decreased collagen production in diabetic rats. Diabetes 37:371–376.

Stein G, Lian J, Owen T. 1990. Relationship of cell growth to the regulation of tissue-specific gene expression during osteoblast differentiation. FASEB J 4:3111–3123.

Stolzing A, Sellers D, Llewelyn O, Scutt A. 2010. Diabetes induced changes in rat mesenchymal stem cells. Cells Tissues Organs 191:453–465.

Suzuki A, Guicheux J, Palmer G, Miura Y, Oiso Y, Bonjour J-P, Caverzasio J. 2002. Evidence for a role of p38 MAP kinase in expression of alkaline phosphatase during osteoblastic cell differentiation. Bone 30:91–98.

Takada I, Kouzmenko A, Kato S. 2009. Wnt and PPARg signaling in osteoblastogenesis and adipogenesis. Nat Rev Rheumatol 5:442–447.

Terada M, Inaba M, Yano Y, Hasuma T, Nishizawa Y, Morii H, Otani S. 1998. Growth-inhibitory effect of a high glucose concentration on osteoblast-like cells. Bone 22:17–23.

Thomsen J, Laib A, Koller B, Prohaska S, Mosekilde L, Gowin W. 2005. Stereological measures of trabecular bone structure: comparison of 3D micro computed tomography with 2D histological sections in human proximal tibial bone biopsies. J Microsc 218:71–179.

Thrailkill KM, Liu L, Wahl EC, Bunn RC, Perrien DS, Cockrell GE, Skinner RA, Hogue WR, Carver AA, Fowlkes JL, Aronson J, Lumpkin CK. 2005. Bone formation is impaired in a model of type 1 diabetes. Diabetes 54:2875–2881.

Tolosa M, Chuguransky S, Sedlinsky C, Schurman L, McCarthy A, Molinuevo M, Cortizo A. 2013. Insulin-deficient diabetes-induced bone microarchitecture alterations are associated with a decrease in the osteogenic potential of bone marrow progenitor cells: preventive effects of metformin. Diabetes Res Clin Pract 101:177–186.

Tullberg-Reinert H, Jundt G. 1999. In situ measurement of collagen synthesis by human bone cells with a Sirius Red-based colorimetric microassay: effects of transforming growth factor β2 and ascorbic acid 2-phosphate. Histochem Cell Biol 112:271–276.

Van Belle TL, Coppieters KT, Von Herrath MG. 2011. Type 1 diabetes: etiology, immunology, and therapeutic strategies. Physiol Rev 91:79–118.

Vestergaard P. 2007. Discrepancies in bone mineral density and fracture risk in patients with type 1 and type 2 diabetes—a meta-analysis. Osteoporos Int 18:427–444.

Wan Y. 2010. PPARγ in bone homeostasis. Trends Endocrinol Metab 21: 722–728.

Wang N, Butler J, Ingber D. 1993. Mechanotransduction across the cell surface and through the cytoskeleton. Science 260:1124–1127.

Wang W, Zhang X, Zheng J, Yang J. 2010. High glucose stimulates adipogenic and inhibits osteogenic differentiation in MG-63 cells through cAMP/protein kinase A/extracellular signal-regulated kinase pathway. Mol Cell Biochem 338:115–122.

Zhang W, Shen X, Wan C, Zhao Q, Zhang L, Zhou Q, Deng L. 2012. Effects of insulin and insulin-like growth factor 1 on osteoblast proliferation and differentiation: differential signalling via Akt and ERK. Cell Biochem Funct 30:297–302.

Zhao Y-F, Zeng D-L, Xia L-G, Zhang S-M, Xu L-Y, Jiang X-Q, Zhang F-Q. 2013. Osteogenic potential of bone marrow stromal cells derived from streptozotocin-induced diabetic rats. Int J Mol Med 31:614–620.

SUPPORTING INFORMATION

Additional supporting information may be found in the online version of this article at the publisher's web-site.